CENTRAL RESEARCH LIBRARY

ORNL-TM-4408

OAK RIDGE NATIONAL LABORATORY LIBRARIES
3 4456 0550279 2

cy.48

EFFECTS OF HIGHLY ANISOTROPIC SCATTERING ON MONOENERGETIC NEUTRON TRANSPORT AT DEEP PENETRATIONS

E. Oblow
K. Kin
H. Goldstein
J. J. Wagshal

OAK RIDGE NATIONAL LABORATORY
CENTRAL RESEARCH LIBRARY
DOCUMENT COLLECTION
LIBRARY LOAN COPY
DO NOT TRANSFER TO ANOTHER PERSON
If you wish someone else to see this document, send in name with document and the library will arrange a loan.
UCN-7969
(3 3-67)

OAK RIDGE NATIONAL LABORATORY
OPERATED BY UNION CARBIDE CORPORATION • FOR THE U.S. ATOMIC ENERGY COMMISSION

This report was prepared as an account of work sponsored by the United States Government. Neither the United States nor the United States Atomic Energy Commission, nor any of their employees, nor any of their contractors, subcontractors, or their employees, makes any warranty, express or implied, or assumes any legal liability or responsibility for the accuracy, completeness or usefulness of any information, apparatus, product or process disclosed, or represents that its use would not infringe privately owned rights.

ORNL-TM-4408

Contract No. W-7405-eng-26

Neutron Physics Division

EFFECTS OF HIGHLY ANISOTROPIC SCATTERING ON MONOENERGETIC NEUTRON TRANSPORT AT DEEP PENETRATIONS†

E. Oblow, K. Kin,* H. Goldstein,*
and J. J. Wagshal**

†Research performed at Columbia University partially supported under subcontract with Union Carbide Corporation for Defense Nuclear Agency under Order 801-70.

*Division of Nuclear Science and Engineering, Columbia University.
**Hebrew University, Jerusalem, Israel.

DECEMBER 1973

OAK RIDGE NATIONAL LABORATORY
Oak Ridge, Tennessee 37830
operated by
UNION CARBIDE CORPORATION
for the
U.S. ATOMIC ENERGY COMMISSION

OAK RIDGE NATIONAL LABORATORY LIBRARIES

3 4456 0550279 2

ABSTRACT

The sensitivity of the flux in deep-penetration problems to anisotropic scattering was studied within the framework of monoenergetic transport theory. Several parameterized, anisotropic scattering kernels were used to represent a general class of anisotropies. The representation of these kernels in Legendre polynomial series of various orders was explored to determine their effect on calculated discrete eigenspectra and infinite medium fluxes. Eigenspectra for several kernels are presented as a function of the kernel parameter. Conclusions were drawn about the order of the Legendre expansion of the kernels required for accurate deep-penetration calculations, and the possible existence of multiple diffusion decay modes in realistic problems. In general, rather low order Legendre expansion was found to be adequate for problems in which the scalar flux was the primary quantity of interest.

TABLE OF CONTENTS

		Page No.
	ABSTRACT	iii
I.	INTRODUCTION	1
II.	THEORY	4
	A. Eigenvalue Equations	4
	B. Methods of Computing Discrete Eigenvalues	6
III.	EIGENSPECTRA FOR PARTICULAR ANISOTROPIES	8
	A. Dirac Delta Functions	8
	B. Gaussian Angular Distributions	15
	C. Realistic Anisotropies	25
IV.	CONCLUSIONS	29

I. INTRODUCTION

The study of anisotropic scattering in neutron transport theory has had a long history, certainly going back at least to Fermi[1] and other early investigations[2,3,4] and lucidly summarized in the monograph by Davison.[5] More recent efforts in this field, notably by Mika[6] and Jacobs,[7] have taken up the method of singular eigenfunctions developed by Case[8] to answer more general questions about the effects of anisotropy. Our specific interest in this problem stems from an investigation of the sensitivity of deeply penetrating neutrons in bulk shields to microscopic cross-section data.[9] The role of scattering anisotropy in such problems, although not as fundamental as that of the total cross section, does raise a number of interesting questions.

Specifically, one would like to know how well fluxes can be calculated using rather poor representations of elastic scattering anisotropies. "Poor" is used here in the sense of low-order expansions of the scattering kernel in Legendre polynomials. Since angular distribution data for shield calculations are often represented in high-order Legendre polynomial series, the effect of truncating such Legendre expansions at very low order needs to be thoroughly investigated if adequate shields are to be designed with a minimum of computing effort. In addition to this consideration, it would also be advantageous to know, in a quantitative way, the behavior of the flux at large distances from a source in highly anisotropic scattering media. The relationship between the roles played by the scattering anisotropy and absorption is important here, as well as the question of their effect on the asymptotic decay of the flux far from any sources.

Due to the relative complexity of shielding design problems, extensive use is made of numerical methods in their solution. This practice necessarily obscures the relationship between the basic microscopic cross-section data and the calculated fluxes. Although more idealized problems are by no means easy to analyze, they certainly simplify matters considerably. We have therefore found it to be more instructive to examine general sensitivity questions in the rather restrictive setting of monoenergetic

transport theory. This approach has the effect of limiting the discussion to transport in the absence of slowing down. Since the effects of anisotropic scattering are evident in both the transport and slowing down processes (arising in the latter case as a result of a coupling between scattering angle and energy loss), this appears to represent a strong limitation of the present approach when applied to general shielding situations. In certain important instances, however, it is felt that conclusions drawn from monoenergetic cases will have more general applicability. From the viewpoint of a multigroup solution of the Boltzmann equation, each group represents a monoenergetic problem with a distributed, anisotropic slowing down source. If, as in the case of a deep-penetration problem, the transport within certain energy groups is of paramount importance and this effect overshadows the effect of the distributed source in these groups, then an analysis of monoenergetic transport can certainly provide useful information in these instances. Such a situation is practically realized in shielding problems using materials where total cross-section behavior contains deep minima or "windows" through which most of the leakage from the shield occurs.

In light of this argument, time-independent monoenergetic transport theory has been used as an analytical tool to answer some specific sensitivity questions. Since deep penetration in bulk shields is our major concern, emphasis is placed on determining the discrete eigenspectrum of the transport operator since it is these discrete modes that are dominant at large distances from any source. As such, the discussion is restricted to an analysis of the scalar flux from a plane isotropic source in an infinite non-multiplying medium. The magnitude of the discrete eigenvalues for this problem will have a direct bearing on both the relaxation length of the flux at large distances from the source and the relative normalization of each eigenmode and thus the amount of deep penetration.

The field of monoenergetic transport theory has been extensively explored in the past. Case[8] pioneered the modern approach of using a complete set of eigenfunctions to describe transport with isotropic scattering. The method was extended by Mika[6] to include the effects of linear

anisotropy and more recently by Jacobs[7] to formally include general anisotropy scattering kernels. Despite these theoretical developments, numerical studies of the discrete root spectrum and answers to sensitivity questions have only appeared in the last few years.[10,11,12] Our efforts are an extension of these latter works and will chiefly be concerned with answering the following three questions:

(1) What is the nature of the discrete eigenspectrum and thus the asymptotic behavior of the flux with a general anisotropic scattering kernel?

(2) How are these eigenvalues and the transport process affected by differing order representations of the scattering kernel in Legendre polynomials?

(3) What effect do such representations have on the scalar flux at large distances from a plane isotropic source in an infinite medium?

As a result of answering these questions we will also shed some light on the possibility of asymptotic flux behavior represented by multiple discrete eigenmodes. Previous work along these lines[6,12] has already given some indication as to the upper limit of the number of discrete modes to expect in certain instances and we will add to this knowledge by dealing with a wider class of anisotropic kernels.

With regard to numerical computations, it should be noted that a number of different techniques for calculating discrete eigenvalues were used to validate all numerical values reported. Intercomparisons of the results from all the methods showed that they were all equally reliable and better than five decimal place precision was achieved in all cases. To maintain consistency only the results from one of the approaches (i.e., the P_L-approximation) were reported unless otherwise indicated. Extensive use of this method of reporting results in comparison with the others was motivated by the fact that the P_L method also provided us with the infinite-medium fluxes needed for other parts of the present work.

II. THEORY

A. Eigenvalue Equations

The monoenergetic transport equation with arbitrary anisotropy when written in homogeneous form in plane geometry serves as the eigenvalue equation for our investigations. In standard form,[13] as a function of the distance in mean free paths, $x = \Sigma_T z$, the equation can be written as:

$$\mu \frac{\partial \psi}{\partial x}(x,\mu) + \psi(x,\mu) = \frac{c}{2} \sum_{\ell} (2\ell + 1) f_\ell P_\ell(\mu) \psi_\ell(x) \tag{1}$$

where

$$\psi_\ell(x) = \int_{-1}^{1} \psi(x,\mu') P_\ell(\mu') d\mu' \tag{2}$$

All other quantities have their conventional meanings.

The characteristic equation for the discrete eigenvalues is generated by assuming a solution Ansatz of the form $\psi(x,\mu) = \phi(\mu) e^{-x/\nu}$ subject to the condition that $|\nu| \geq 1$. If this solution form is inserted into Eq. (1) and a normalization condition used on the integral of $\phi(\mu)$, we can identify a function $\Lambda(\nu)$ whose zeros represent the discrete eigenvalues, as follows:

$$\Lambda(\nu) = 1 - \frac{c\nu}{2} \sum_{\ell}^{\infty} (2\ell + 1) f_\ell \phi_{\nu\ell} Q_\ell(\nu) \quad . \tag{3}$$

The $\phi_{\nu\ell}$'s here are Kuščer polynomials [physically the angular moments of $\phi(x,\mu)$ in the νth mode], which are functions of c and the f_ℓ's. These polynomials can be generated from the following recursion relationship:

$$\nu(1 - cf_\ell) \phi_{\nu\ell} = \frac{\ell + 1}{2\ell + 1} \phi_{\nu,\ell+1} + \frac{\ell}{2\ell + 1} \phi_{\nu,\ell-1} \qquad \ell=0,1,\ldots\infty \tag{4}$$

The $Q_\ell(\nu)$'s are Legendre functions of the second kind defined as follows:

$$Q_\ell(\nu) = \frac{1}{2} \int_{-1}^{1} \frac{P_\ell(\nu)}{\nu - \mu} d\mu \qquad |\nu| \geq 1 \quad . \tag{5}$$

For each discrete eigenvalue in Eq. (3) there is an associated discrete eigenfunction, which together with the continuum eigenfunctions (associated with the eigenvalues $|\nu| \leq 1$) form a mathematically complete set in μ space in a number of practical instances. The problem of a plane isotropic source in an infinite medium is such a case, amenable to solution with a set of eigenfunctions complete over the full angular range $-1 \leq \mu \leq 1$. In this instance we can write the solution for $x > 0$ as follows:

$$\psi_\ell(x) = \sum_{j=1}^{J} A_{\nu_j} \phi_{\nu_j,\ell} \, e^{-x/\nu_j} + \int_0^1 A(\nu) \, \phi_\ell(\nu) \, e^{-x/\nu} \, d\nu \qquad x > 0 \tag{6}$$

where the $\phi_{\nu,\ell}$ and $\phi_\ell(\nu)$ are the angular moments of the discrete and continuum eigenmodes, respectively, and the A_{ν_j} and $A(\nu)$ are the eigenmode normalization coefficients, which are completely determined by a jump boundary condition at the source plane.[13]

The historical approach to solving Eq. (1) has been the P_L method. Both sides of the equation are first multiplied by $P_\ell(\mu)$ and integrated over μ from -1 to 1. The infinite set of equations (for all ℓ values) which results is then truncated at ℓ=L by setting $\partial\psi_{L+1}(x)\partial x = 0$. This gives rise to the finite P_L-approximation equations, a series of coupled linear first-order differential equations which are also solvable with an Ansatz of the form $\psi(x,\mu) = \phi(\mu) \, e^{-x/\nu}$. As L approaches infinity the procedure above results in an infinite set of equations which are an alternate representation of Eq. (1). The P_L-approximation solution for L approaching infinity thus converges to the rigorous one.[5] In particular, the continuum eigenfunctions in this limit are approximated by an infinite set of discrete values lying in the range $-1 \leq \nu \leq 1$. This alternate approach to solving the monoenergetic problem also yields results for discrete mode eigenvalues and normalization coefficients and is thus quite useful for numerically approximating rigorous solutions.

B. Methods of Computing Discrete Eigenvalues

Having presented the characteristic eigenvalue equation, a brief discussion of the numerical methods by which it was solved is now in order. Since the equation is trancentental in ν it is impossible to get an **explicit** analytic representation of all the roots; numerical approximations must be employed. In computing these values use can be made of the fact that the eigenvalues always appear in pairs as $\pm\,|\nu|$.[13] We will therefore limit ourselves in what follows to a discussion of positive roots only and flux solutions for $x > 0$.

In a straightforward manner, one of the methods used to evaluate the eigenspectrum involves a direct procedure for determining the zeros of $\Lambda(\nu)$ in Eq. (3). To accomplish this, a coarse scan of a region in ν space from $0 \leq |\nu|^{-1} \leq 1$ is made in search of points at which $\Lambda(\nu)$ changes sign. Once these values of ν are located, a suitable convergence scheme is used to get the root to any degree of precision desired. The $Q_\ell(\nu)$ functions in this instance are calculated by backward recursion relationships starting at ℓ=L so as to minimize roundoff errors. The value of $Q_L(\nu)$ needed to initiate this recursion is obtained from its definition in terms of hypergeometric functions,[14] which in turn are calculated from a polynomial series in ν^{-2}. Calculation of the $\phi_{\nu\ell}$'s also makes use of a recursion relationship, specifically that given in Eq. (4).

A second approach to solving Eq. (3), due to Van de Hulst,[12] was also employed. Here use is made of the fact that the ratio of Kuscer polynomials of order ℓ and ℓ+1 is given by the following simple recursion relationship:

$$r_\ell(\nu) = \frac{\ell}{(2\ell+1)(1-cf_\ell)\nu - (\ell+1)r_{\ell+1}(\nu)} \tag{7}$$

where $r_{\ell+1}(\nu) \equiv \phi_{\nu,\ell+1}/\phi_{\nu,\ell}$. For ℓ=1, $\ell=\infty$, and ℓ=L+1 (where $f_\ell \equiv 0$ for all ℓ>L), the following particularly simple relationships exist:

$$r_1(\nu) = (1 - c)\nu \tag{8}$$

$$r_\infty(\nu) = \nu - \sqrt{\nu^2 - 1} \tag{9}$$

and

$$r_{L+1}(\nu) = r_\infty(\nu) \left[1 - \frac{1}{2(L+1)} + \text{error of order} \left(\frac{1}{(L+1)^2} \right)\right] \quad . \tag{10}$$

Using these results, the Van de Hulst approach suggests the following root-finding scheme: (a) scan the ν range and compute a value of $r_\infty(\nu)$ for each value of ν; (b) use $r_\infty(\nu)$ to get an approximate value of $r_{L+1}(\nu)$ using Eq. (10); (c) use Eq. (7) and the set of f_ℓ's $\ell \leq L$ to recurse backwards to $r_1(\nu)$; and (d) compare the new value of ν obtained from Eq. (8) with the one guessed at to begin the scan. This process is continued until the guessed value is approximately equal to the recursed value, at which point the result can be made as precise as desired using any convenient numerical root-finding scheme. Van de Hulst points out that the recursion error decreases as $1/r_\infty^2$ in each backward step (r_∞ being less than unity), while forward recursion errors increase as r_∞^2.

As a way of checking that no roots are missed in the scan, Van de Hulst also suggests that for a series of fixed ν values, one can solve the eigenvalue equation for L values of c. With ν known, Eq. (3) is simply an Lth-order polynomial equation in c with L roots. Plotting the L values of c which solve the equation as a function of ν it is quite easy to check the exact number of ν roots for any particular c value by observing how many curves have intersections with the chosen c value. This reverse procedure points out the fact that the number of ν roots is always less than or equal to L, the maximum order f_ℓ used to represent the scattering kernel. There are at most L curves which can produce crossings, and thus eigenvalues, as a function of ν.

A third approach to the eigenvalue problem involved the use of the traditional P_L approximation.[16] For very large L, as we have already

pointed out, this method yields solutions which approach the rigorous results. The eigenvalues obtained are thus converged to any desired precision by increasing the order of the approximation. In practice, approximations of order L = 39 were found to be quite satisfactory for the types of anisotropies investigated. Since the P_L-method with odd L yields [(L+1)/2] distinct pairs of eigenvalues including a discrete representation of the continuum $|\nu| \leq 1$, the actual discrete eigenvalues are identified as those with $|\nu| \geq 1$. Although the calculation of these discrete values cannot be separated from a determination of roots with $|\nu| \leq 1$, there is little difficulty in calculating all the eigenvalues by QR double iteration.[17] For L not too large (about 39) the procedure, in fact, is somewhat less time consuming than the scanning techniques used. The accuracy of all the methods used, in any event, compared favorably for all the problems studied. In general there was little difficulty in obtaining five-decimal place precision for all eigenvalues with all three methods.

III. EIGENSPECTRA FOR PARTICULAR ANISOTROPIES

In order to determine the sensitivity of the flux to anisotropic scattering and also to shed some light on the transport process with highly forward peaked anisotropies, a number of functional representations of the scattering kernel in parametric form were chosen for study. This approach allows the calculation of eigenspectra and the identification of effects to be made as a function of a single parameter at a time. The investigation includes a detailed discussion of the discrete eigenspectra of several anisotropies as a means of explaining flux sensitivity effects and determining the modes of transport at deep penetration.

A. Dirac Delta Functions

Probably the most illustrative single-parameter anisotropy is one of the form $\delta(\mu-\mu_o)/2\pi$, where $\delta(\mu)$ is a Dirac delta function. With a function of this type all scattering is restricted to the surface of a cone of angle whose cosine is μ_o with respect to the x axis. The particular case of

$\mu_o=1$ is most interesting and merits some examination. In this instance scattering is in the forward direction only, with the result that there is no net change in the direction of the transporting particle. Under such conditions the process can be likened to one in which particles transport in a purely absorbing medium -- scattering events having no effect on transport. This analogy is particularly useful in that the problem of transport in a purely absorbing medium has an analytical solution for the flux (it is simply unscattered). Numerical calculations using this delta function anisotropy can therefore be compared with theoretical predictions. In addition to this fact, we can speak of such an anisotropic angular distribution in a limiting sense as a "worst" kind of anisotropy. It is approached but never reached in many real situations (for instance, as neutron energies increase the scattering anisotropy in any nuclide becomes increasingly forward peaked). The results for this case should therefore provide an upper bound to the kinds of effects likely to be found in practical situations.

With regard to the eigenspectrum arising from such an anisotropy, it should be noted that the spectrum in a purely absorbing system consists solely of a continuum in the range $0 \leq |\nu| \leq 1$. No discrete modes exist and the plane geometry flux in all eigenmodes decays faster than $e^{-\Sigma_T z}$. For the delta function anisotropy we can therefore expect on theoretical grounds that the eigenspectrum will approximate a continuum as the number of f_ℓ's used approaches infinity. In this instance the value of c acts as an arbitrary scale factor (since scattering has no effect on transport) extending the continuum range $0 \leq |\nu| \leq (1-c)^{-1}$. The upper limit in this case is the natural upper limit for any non-multiplying system since the flux can decay no slower than $e^{-\Sigma_T z}$ and $\Sigma_T z(1-c) = \Sigma_A z$.

Clearly then for this extreme case of anisotropy, the discrete part of the eigenspectrum from $1 \leq |\nu| \leq (1-c)^{-1}$ goes over into a continuum. Using a finite number of f_ℓ's to represent the anisotropy, however, generates only a finite number of discrete eigenvalues. The continuum is therefore approximated by a denumerable infinity of discrete roots as order

of the approximation approaches infinity. Since we always deal with a truncated series of f_ℓ's and a finite discrete eigenspectrum in any realistic calculation, the success of the truncation in approximating the theoretical case can only be judged by comparing fluxes in this instance. It is meaningless to make any statement about how well discrete roots approximate a continuum. For other $\delta(\mu-\mu_o)$ anisotropies, where $\mu_o \neq 1$, a finite order discrete eigenspectrum was found to exist and for these cases (specifically for $\mu_o = 0.8$ and 0.9) the effect of truncations on the eigenvalues can be evaluated.

The $\delta(\mu-1)/2\pi$ anisotropy was therefore chosen to begin the study of determining the effect of different order Legendre series representations on the infinite medium flux from a plane isotropic source. All the f_ℓ's in this case are unity and a value of c=0.5 was arbitrarily chosen for use in all the runs since c appears only as a scale factor in the analytic flux solution for this case.

Some striking conclusions about how well a forward peaked delta function anisotropy can be approximated with just a relatively low-order series of f_ℓ's, with ℓ in the range $0 \leq \ell \leq \ell_{max}$, is illustrated in Table 1 and Fig. 1. The table and the figure show the eigenspectra and infinite medium scalar fluxes, respectively, resulting from a series of $\delta(\mu-1)/2\pi$ anisotropy runs with c=0.5 using several values of ℓ_{max} from 3 to 36 in a P_{39}-approximation calculation.

The fact that the approximation of the infinite series of f_ℓ's by a finite number of them results in a finite discrete spectrum approximation to the continuun is clear from Table 1. As ℓ_{max} increases, more discrete roots appear to fill up the region from $|\nu|=1$ to $|\nu|=(1-c)^{-1}$. Although these approximate eigenspectra will never represent the continuum, they approximate this behavior in the same way that a finite order P_L-approximation with a finite number of eigenvalues represents the portion of the continuum with $|\nu| \leq 1$. That is to say, the discrete eigenspectrum spans the whole range of the continuum, becoming denser as the order of approximation increases and the scalar flux for any particular problem

Table 1. Discrete Eigenspectrum for $\delta(\mu-1)2\pi$ Anisotropy with c=0.5 as a Function of Highest Order f_ℓ Used in a P_{39}-Approximation Calculation

	ν_1	ν_2	ν_3	ν_4	ν_5	ν_6	ν_7	ν_8	ν_9	ν_{10}	ν_{11}	ν_{12}	ν_{13}
f_3	1.7654	1.0263	-	-	-	-	-	-	-	-	-	-	-
f_6	1.9077	1.5387	1.0205	-	-	-	-	-	-	-	-	-	-
f_9	1.9313	1.7495	1.4129	1.0171	-	-	-	-	-	-	-	-	-
f_{12}	1.9700	1.8442	1.6268	1.3348	1.0147	-	-	-	-	-	-	-	-
f_{15}	1.9797	1.8941	1.7438	1.5359	1.2818	1.0129	-	-	-	-	-	-	-
f_{18}	1.9854	1.9234	1.8138	1.6601	1.4672	1.2435	1.0116	-	-	-	-	-	-
f_{21}	1.9889	1.9421	1.8588	1.7409	1.5914	1.4139	1.2145	1.0105	-	-	-	-	-
f_{24}	1.9914	1.9547	1.8893	1.7963	1.6774	1.5348	1.3714	1.1917	1.0095	-	-	-	-
f_{27}	1.9931	1.9636	1.9109	1.8358	1.7392	1.6226	1.4876	1.3368	1.1734	1.0085	-	-	-
f_{30}	1.9943	1.9701	1.9268	1.8648	1.7849	1.6880	1.5752	1.4479	1.3080	1.1583	1.0074	-	-
f_{33}	1.9952	1.9750	1.9333	1.8868	1.8197	1.7380	1.6425	1.5341	1.4141	1.2838	1.1457	1.0055	-
f_{36}	1.9960	1.9788	1.9480	1.9099	1.8467	1.7770	1.6952	1.6020	1.4982	1.3848	1.2629	1.1341	1.007

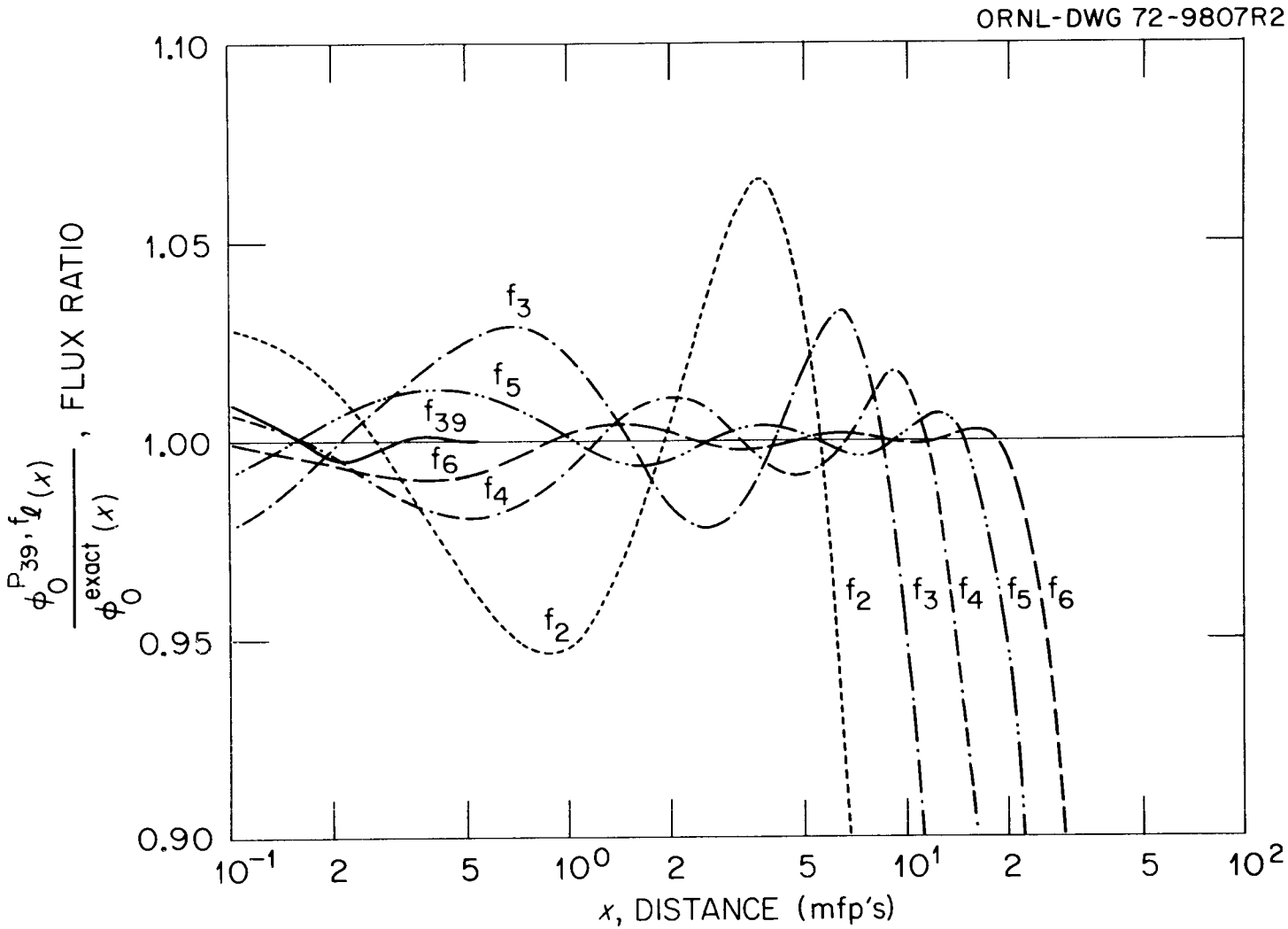

Fig. 1. Comparison of P_{39}-Approximation Scalar Fluxes from Different f_ℓ Truncations of a $\delta(\mu-1)$ Anisotropy with Exact Results for a Plane Isotropic Source in an Infinite Medium.

may be represented to a high degree of precision in any event. This fact is borne out in the comparisons of approximate and rigorous fluxes shown in Fig. 1.

From theoretical considerations, the scalar flux from a plane isotropic source in an infinite, purely absorbing medium is known to behave as $E_1(\Sigma_A z)$ (i.e., as an exponential integral of the first kind). Figure 1 shows a comparison of the scalar flux in a c=0.5 medium resulting from a P_{39}-approximation with a $\delta(\mu-1)/2\pi$ anisotropy and rigorous $E_1(0.5\ x)$ results for varying values of ℓ_{max}. It is clear that even an $\ell_{max} = 3$ truncation of the series is sufficient to give results within 4% of the rigorous E_1 behavior in a range from 0.1 mfp to 10 mfp. This is quite remarkable since the E_1 function is singular at the x=0 source plane and behaves as $x^{-1}\ e^{-(1-c)x}$ at large values of x. With higher values of ℓ_{max} we see that the oscillatory nature of the errors decreases, and together with this, the range over which the approximation is satisfactory increases substantially. Thus more discrete roots, with the largest approaching $|\nu|=(1-c)^{-1}$ and the smallest approaching $|\nu|=1$, result in a better approximation to the behavior of the scalar flux at large and small distances from the source. The fact that an $E_1(x)$ is singular at the origin and goes as $x^{-1}\ e^{-(1-c)x}$ at very large x will, however, always result in a breakdown of the approximation in these regions for any finite number of f_ℓ's.

To all intents and purposes, however, it is safe to conclude that an f_3 truncation ($\ell_{max} = 3$), yielding scalar fluxes within 4% of the rigorous values out to 10 mfp, is a reasonable approximation for this case. The argument is further substantiated when a comparison of rigorous and approximate angular fluxes is made. The representative sampling of results shown in Table 2 illustrate the comparison of rigorous angular fluxes for this case (given as $e^{-[x/\mu(1-c)]}$ for $x/\mu>0$ and zero otherwise)[5] and the results for an f_3,P_{39}-calculation. The f_3 truncated angular flux is also a good approximation to the forward peaked nature of the rigorous behavior.

Looking at the convergence of the numerical values of the discrete roots of other delta function anisotropies gives further evidence for the

Table 2. Comparison of Infinite Medium Angular Fluxes at Representative Angles and Space Points with Exact (E) and f_3, P_{39}-Approximation Calculations (C) for a $\delta(\mu-1)/2\pi$ Anisotropy and c=0.5

mfp \ μ		0.2	0.4	0.6	0.8	1.0
0.1	C	2.444(-1)*	1.668(-1)	1.118(-1)	8.592(-2)	8.554(-2)
	E	2.413(-1)	1.549(-1)	1.123(-1)	8.779(-2)	7.200(-2)
0.5	C	2.790(-2)	5.7333(-2)	5.959(-2)	5.115(-2)	5.218(-2)
	E	3.247(-2)	5.682(-2)	5.752(-2)	5.317(-2)	4.823(-2)
1.0	C	4.234(-3)	1.455(-2)	2.511(-2)	2.890(-2)	2.912(-2)
	E	2.681(-3)	1.633(-2)	2.506(-2)	2.850(-2)	2.928(-2)
5.0	C	-5.902(-7)	7.217(-7)	3.637(-5)	1.808(-4)	5.532(-4)
	E	5.209(-12)	7.195(-7)	3.125(-5)	1.892(-4)	5.299(-4)
10	C	2.484(-8)	-5.388(-8)	-6.543(-8)	5.239(-7)	3.176(-6)
	E	7.674(-23)	2.763(-12)	7.662(-9)	3.708(-7)	3.613(-6)

*Read: 2.444×10^{-1}, etc.

success of low-order truncations. As an illustration, the convergence of the largest discrete eigenvalue in the spectrum of delta functions with μ_o = 0.8 and 0.9 for a c=0.5 medium is presented in Table 3. It is clear that using only an f_3 truncation this eigenvalue is converged to better than 0.2% in both cases. Considering the fact that the second largest eigenvalues (ν_2 = 1.05049 and 1.08150 for the μ_o = 0.8 and 0.9 cases respectively) are well separated from the largest, the total scalar flux at large distances from the source will be dominated by the largest eigenvalue mode. A 0.2% error in the decay rate of the asymptotic mode will therefore not appreciably effect the flux until distances greater than 20 mean free paths.

A discussion of why such low-order expansion work so well will be left for the final section of this paper. For now, we will try to illustrate in a bit more detail the same kinds of results for more realistic anisotropies seeing how they compare with the extreme cases of the delta functions.

B. Gaussian Angular Distributions

To represent more realistic angular distributions and still retain a parameterized functional form which will be able to cover isotropic as well as forward peaked distributions, a gaussian of the following form was used:

$$f(\mu) = A\, e^{-[(\mu-\mu_o)/\beta]^2} \qquad -1 \leq \mu,\mu_o \leq 1 \quad . \tag{11}$$

In the limit as $\beta \to 0$ the distribution approaches delta function behavior at $\mu=\mu_o$, as $\beta \to \infty$ the distribution becomes isotropic, and for β values in between various other angular distributions can be formed.

The particular case of μ_o=1 with various values of β and c offers a convenient extension of the work with the forward peaked delta function. This case also gives a strong indication of the type of realistic

Table 3. Largest Discrete Eigenvalue of $\delta(\mu-\mu_o)/2\pi$ Anisotropy with c=0.5 and Various f_ℓ Truncations as a Function of ℓ_{max} and μ_o

ℓ_{max} \ μ_o	0.8	0.9
0	1.04438	1.04438
1	1.28854	1.34086
2	1.35926	1.47348
3	1.36258	1.50297
4	1.36088	1.50607
5	1.36050	1.50597
6	1.36046	1.50590
7	1.36045	1.50589

anisotropy likely to yield a multiplicity of discrete roots and their effects on transport. Figures 2 and 3 summarize the first part of the results with this angular distribution in the form of plots of eigenvalues vs β and c variation. Figure 2 shows the eigenspectrum variation as a function of β for a c=0.8 case and Fig. 3 shows the variation as a function of c for a β=0.1 case.

A look at Fig. 2 reveals that such gaussian anisotropies can give rise to true multiple discrete-root spectra. The multiplicities are seen to range from two up to eight as the angular distributions become increasingly forward-peaked (i.e., as β decreases). For this c=0.8 case, for example, the multiplicity is three for a gaussian of width β=0.1 and eight with β=0.01. These results indicate that the more forward peaked the angular distribution the greater the multiplicity of the roots in the discrete spectrum.

The fact that greater multiplicities are also correlated with larger scattering probabilities (as measured by $c=\Sigma_s/\Sigma_T$) is illustrated in Fig. 3. Here we see that for a β=0.1 gaussian a second eigenvalue appears for c values greater than 0.264. The values of the first and the second roots increase monotonically with increasing values of c until a third root appears at c=0.734. All three roots then increase in magnitude until at c=1 we get ν_1^{-1}=0.0, ν_2^{-1}=0.37, and ν_3^{-1}=0.83. Since at least two roots are present when c=0.5 (approximately the c value for fast neutron interactions), these results indicate that under somewhat realistic conditions two discrete diffusion modes may be present.

As a result of further runs with μ_o = 0.0 and -1.0, and various other β and c values, we generally concluded that multiple discrete eigenvalues do exist with highly anisotropic distributions in media with even small c values. A high degree of scattering anisotropy, however, does appear to be a definite prerequisite for such additional engenmodes to occur. Also, the more forward peaked the anisotropy the larger the multiplicity will be for any given β and c values.

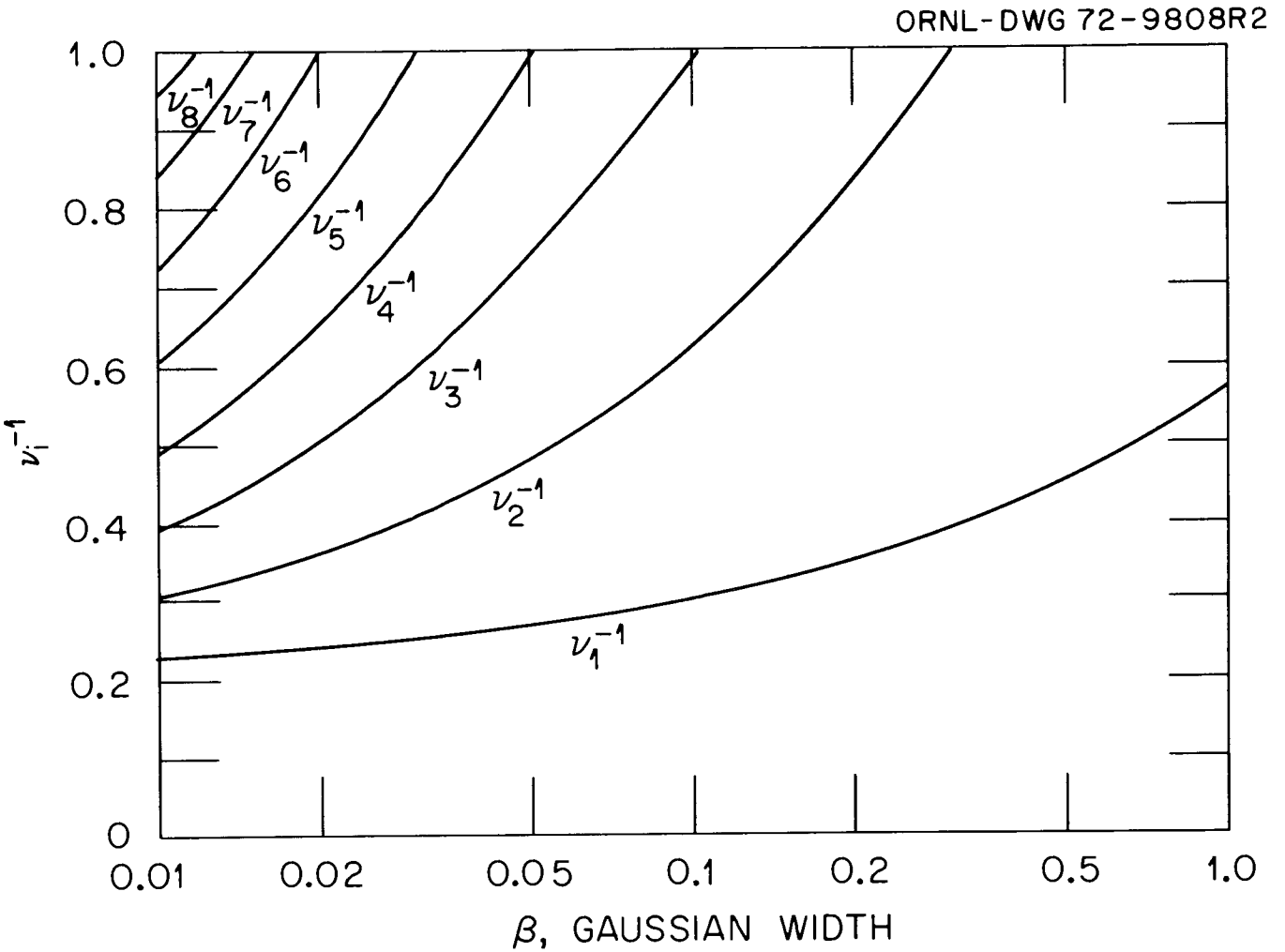

Fig. 2. Discrete Eigenspectrum for Gaussian Anisotropy with c=0.8 as a Function of β from a P_{39},f_{39} Calculation.

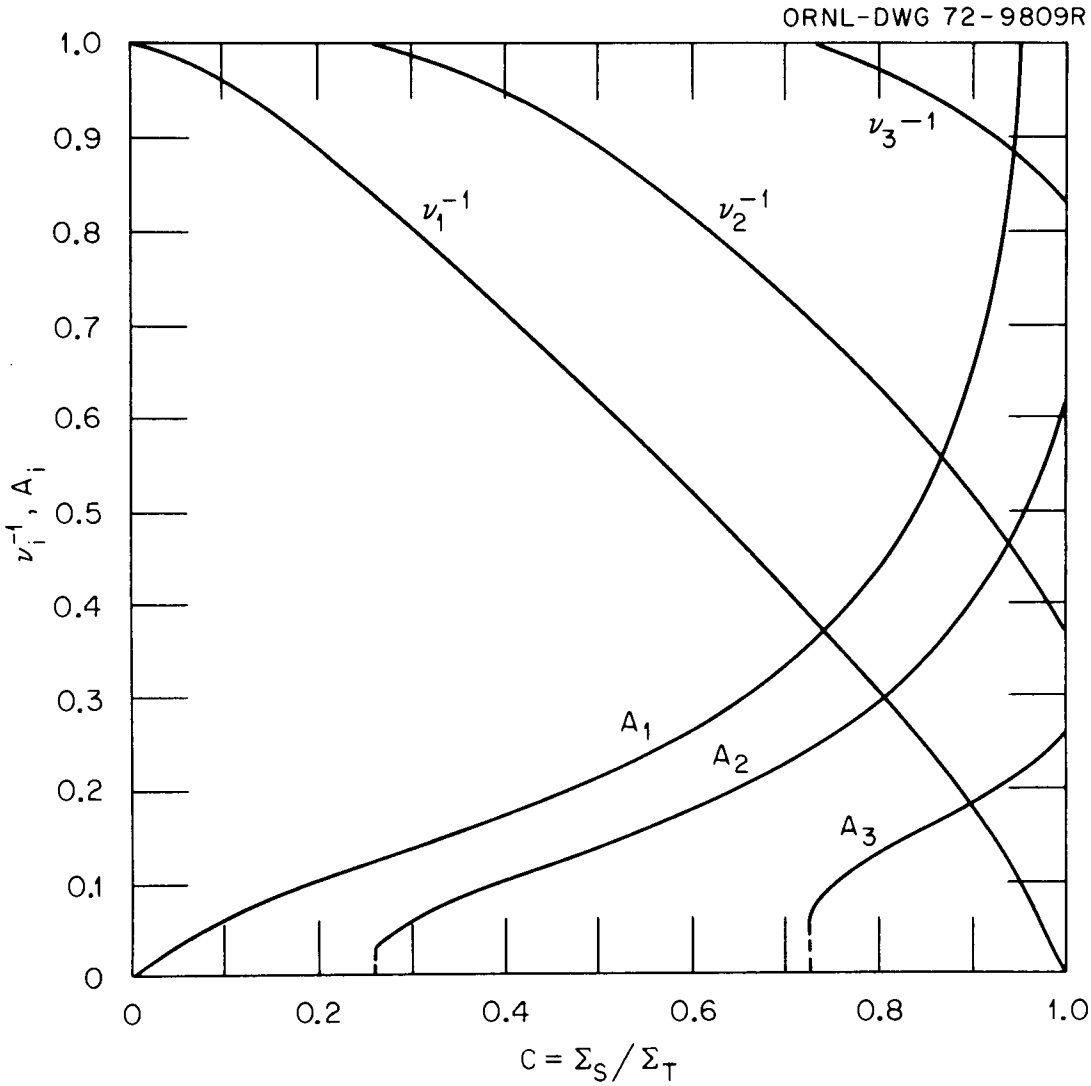

Fig. 3. Discrete Eigenspectrum and Plane Isotropic Source, Infinite Medium Eigenfunction Coefficients for a Gaussian Anisotropy with β=0.1 as a Function of c from a P_{39},f_{39} Calculation.

Further conclusions, which concur with those obtained for delta function scattering, can also be drawn about truncations of the infinite f_ℓ series for this anisotropy. These results give valuable information about how well approximate solutions to the transport equation can be expected to agree with rigorous results. Again, the accuracy of the eigenvalues has a major bearing on how good any approximation is. In Fig. 4, for instance, the errors in the three roots which arise in β=0.1, μ_o=1, c=0.8 case show that with an f_8 truncation all three roots have appeared and are within 0.5% of their fully converged values. In fact, with only an f_5 truncation the two largest roots have already appeared and are converged to within 0.5% (for an f_3 case the largest root is good to three place precision). Thus for very deep penetration ($\sim$ 10 mfp's) where only the largest root will be important, a third order expansion of the angular distribution in Legendre polynomials should give the decay rate of the flux to within 0.1%.

When the actual scalar flux is calculated and these truncation approximations are compared with fully converged results, the success of low-order expansions becomes even more apparent. The effect on the scalar flux of truncating a gaussian anisotropy with β=0.1, μ_o=1.0, and c=0.5 is shown in Fig. 5. Here, in comparison with the forward peaked delta function results of Fig. 1, we see that an f_5 expansion for the gaussian yields more accurate fluxes on a point-by-point basis as a function of distance. Note that the f_5 and f_6 curves produce ratios which are almost unity from 10 mfp's onward in Fig. 5. The improvement is such that accuracies to within 0.4% in a region extending well out to 100 mfp's, are achieved with an f_5 expansion for the gaussian, while 1.5% accuracy, out to only 15 mfp's is obtained with the same truncation for the delta function. The accuracy in either case is certainly sufficient for practical problems but the increased range of agreement for the gaussian case indicates that even very deep penetration problems (> 10 mfp's) will be handled quite easily with an f_5 expansion.

One of the surprising results derived from a study of this anisotropy is related to the effect of multiple discrete roots on moderate and deep

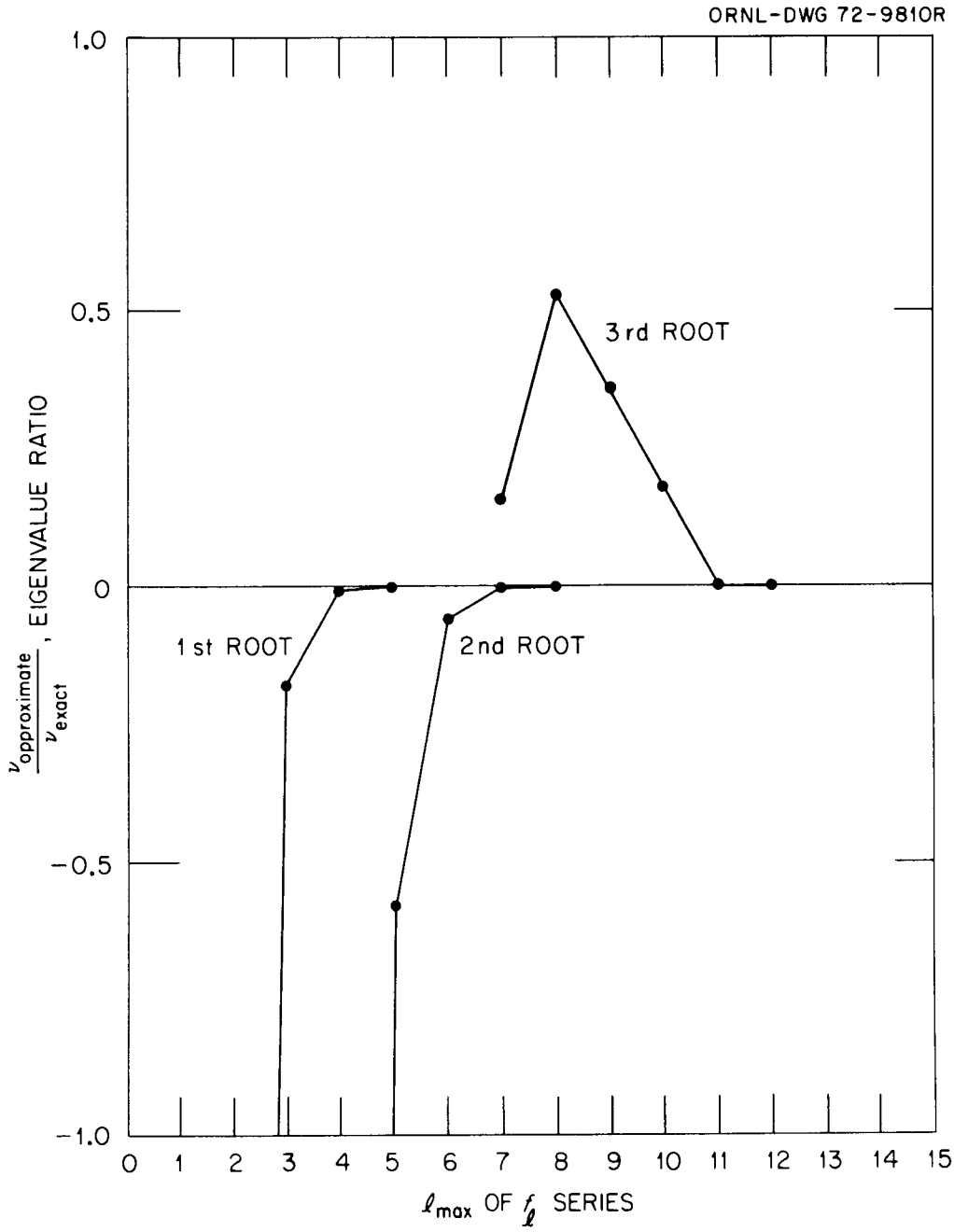

Fig. 4. Comparison of Eigenvalues from a Truncated f_ℓ Series and Exact Values for a Gaussian Anisotropy with β=0.1 and c=0.8 as a Function of ℓ_{max}.

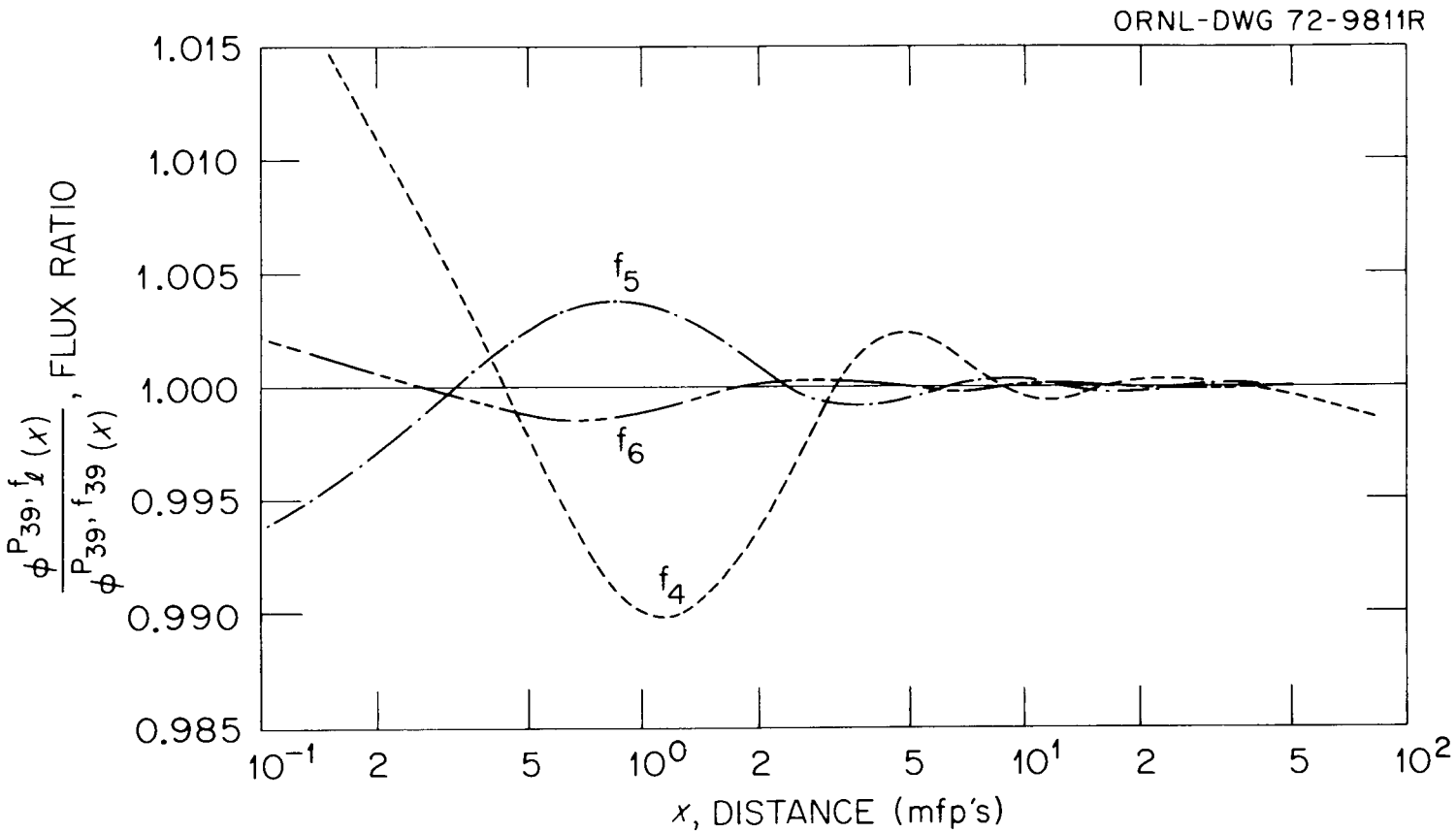

Fig. 5. Comparison of P_{39}-Approximation Scalar Fluxes from Different f_ℓ Truncations of a Gaussian Anisotropy ($c=0.8$ and $\beta=0.1$) with a P_{39}, f_{39} Scalar Fluxes for a Plane Isotropic Source in an Infinite Medium.

penetration calculations. One might at first glance assume that even though multiple roots would be theoretically possible, the coefficients associated with each eigenmode would be such that only the mode with the largest eigenvalue would make a substantial contribution to the scalar flux. This appears not to be the case, as is illustrated in one of the previous figures, Fig. 3, and also in Fig. 6. The coefficients for each eigenmode in the case of a gaussian anisotropy with β=0.1, μ_o=1.0, and various c values are shown back in Fig. 3, while the contribution of each mode to the total scalar flux from a plane isotropic source in an infinite medium with c=0.8, appears in Fig. 6.

What is apparent here is that the relative strengths of each mode (as determined by the A_ν values) are quite comparable in all cases except as c approaches unity. Certainly for the c=0.8 case, as illustrated in Fig. 6, one has to go at least 3 mfp away from the source before the contribution of the third and weakest mode drops below 3%. A distance of 8 mfp is needed before the contribution of the second mode drops below this value. In a spatial region close to the source where the continuum eigenmodes are usually very important, the three discrete modes contribute roughly in proportion to the size of their coefficients. For x=1 this results in about 8% of the total flux being in the third mode, 23% in the second mode, and 50% in the first mode. The effect of multiple diffusion-type transport modes is thus significant over a wide range of space. Certainly these modes contribute substantially to the flux at moderate distances (1-3 mfp) and while their effect on deeper penetrations (beyond 5 mfp) is not too large, it certainly is not negligible as one might have expected.

It is interesting to note at this point that the contributions of the additional discrete modes is relatively large compared with the much discussed "transient" component of the flux. For the case above, for instance, less than 15% of the flux at x=1.0 is in the transient mode. This is small in comparison with the over 30% contribution of the second and third discrete modes combined. With increasing values of c the transient becomes even less significant, in addition to the fact that it dies out more quickly

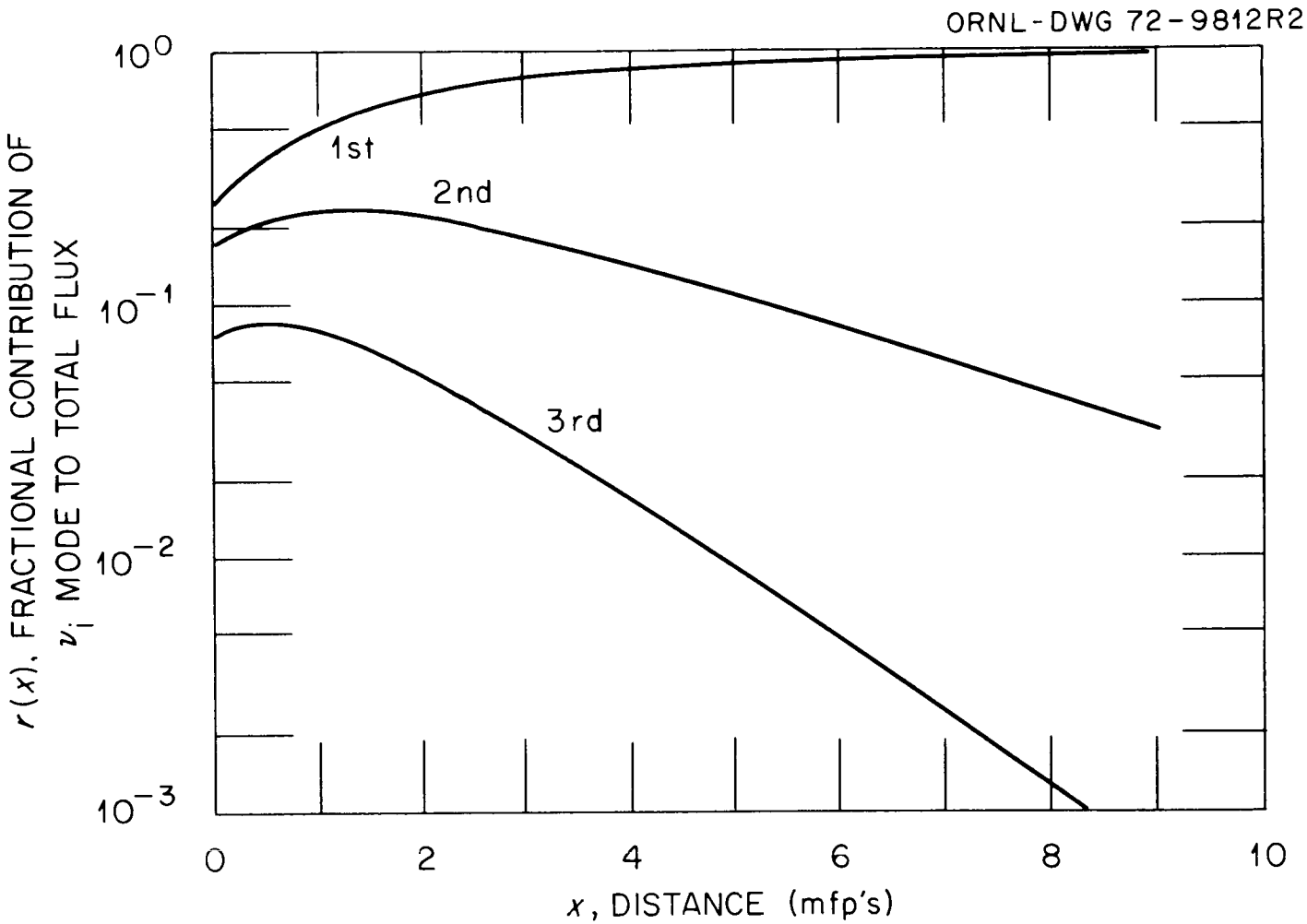

Fig. 6. The Ratio of Each Discrete Eigenmode's Contribution to the Total Infinite Medium Flux for a Gaussian Anisotropy with c=0.8 and β=0.1 from a P_{39},f_{39} Calculation.

the larger the value of c.[13] Only in cases with $c < 0.5$ does the transient play a larger role than the additional discrete modes for this case.

C. Realistic Anisotropies

As a final way of demonstrating the effects of highly anisotropic scattering on transport, we will consider two cases of forward peaked anisotropies found in the nuclides ^{208}Pb and ^{338}U. The angular distributions for ^{208}Pb at 14.5 MeV[15] and ^{238}U at 14.1 MeV[15] with f_ℓ's as given in Table 4 were chosen for this study. In both instances, the angular distributions have a large forward-peaked component (comparable to a gaussian of width β=0.1), as well as diffraction peak structure at smaller angles. Because of the behavior near μ=1.0, however, we can expect the eigenspectra in both cases to look very much like that of a β=0.1 gaussian and indeed the results shown in Figs. 7 and 8 bear this out. Figure 7 shows the eigenvalues and eigenmode coefficients as a function of c for the ^{208}Pb anisotropy and Fig. 8, the comparable result for the ^{238}U case.

Here we have a clear demonstration that multiple diffusion-type models are indeed possible for the fast neutron anisotropies found in heavy materials. Furthermore, a comparison of Fig. 2 and Figs. 7 and 8 brings out the fact that the most important qualitative feature of the angular distribution for this occurrence is its behavior near μ=1. Both the ^{208}Pb and ^{238}U differential scattering cross sections have sharply peaked forward scattering components with half-widths around μ=1 of about 0.1, the ^{208}Pb distribution in this case being a bit narrower than that of ^{238}U. As the figures show, the ^{208}Pb has up to four discrete roots and the ^{238}U up to three for highly scattering media (c approaching unity). These multiplicities as a function of c are qualitatively comparable to those found with the gaussian of width β=0.1.

For flux calculations the relative magnitudes of the A_ν's are important, and here again the results are comparable to those found for the gaussian case. The ^{208}Pb eigenspectrum is somewhat more dominated by the largest ν mode than the ^{238}U spectrum and for c=1 the fourth root plays as important a role as the third for the former nuclide.

Table 4. Legendre Expansion Coefficients for 14.1-MeV ^{238}U and 14.5-MeV ^{208}Pb Elastic Scattering Angular Distributions in Laboratory System

	Lead (14.5 MeV)	Uranium (14.1 MeV)
f_0	1.0	1.0
f_1	0.8462	0.8937
f_2	0.7074	0.7793
f_3	0.5745	0.6595
f_4	0.4808	0.5425
f_5	0.4045	0.4349
f_6	0.3502	0.3366
f_7	0.3056	0.2490
f_8	0.2668	0.1735
f_9	0.2273	0.1080
f_{10}	0.1546	0.0557
f_{11}	0.0971	0.0137
f_{12}	0.0466	-0.0212
f_{13}	0.0129	-0.0437
f_{14}	0.0051	-0.0517

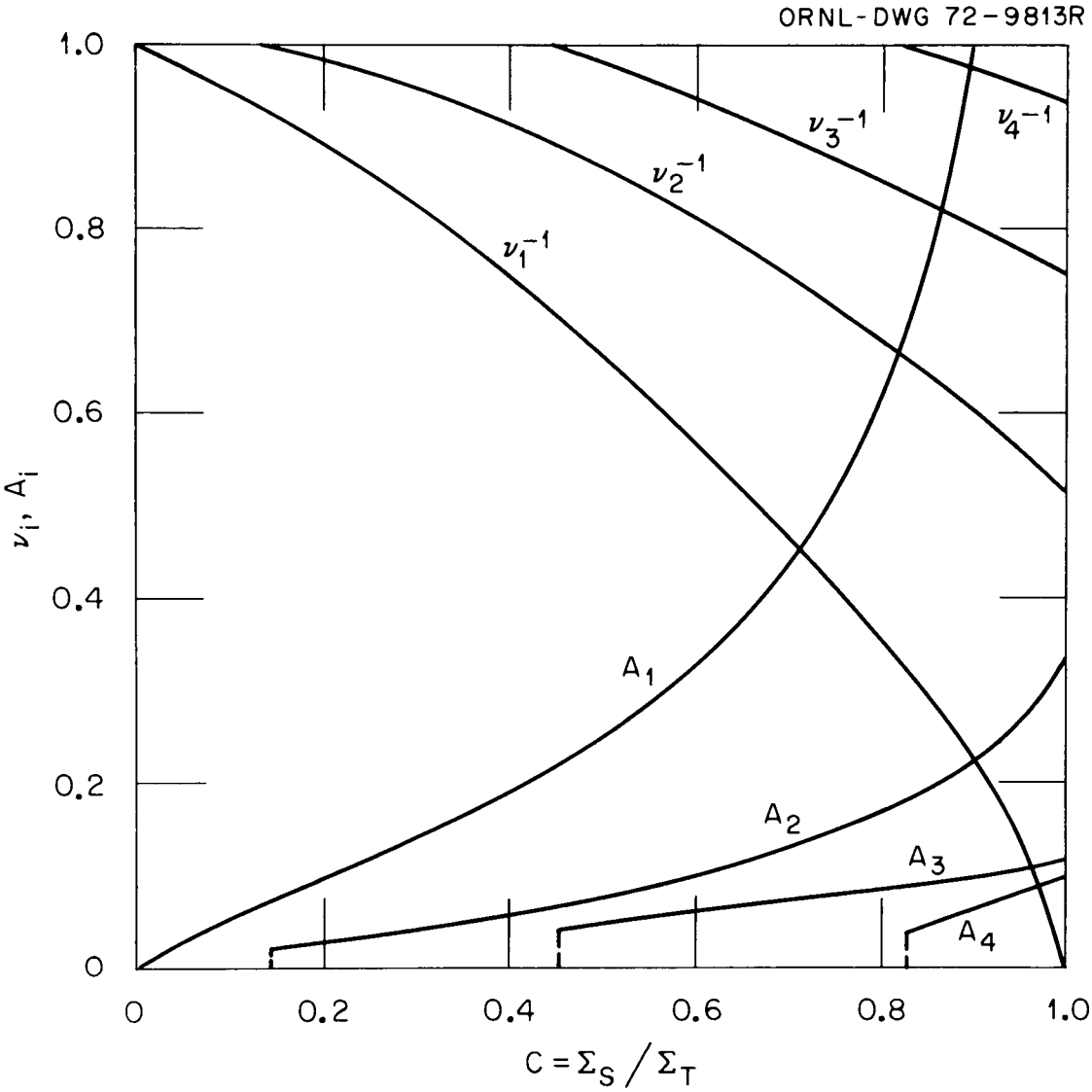

Fig. 7. Discrete Eigenspectrum and Infinite Medium Flux Eigenfunction Coefficients from the ^{208}Pb 14.5-MeV Angular Distribution as a Function of c, from a P_{39},f_{14} Calculation.

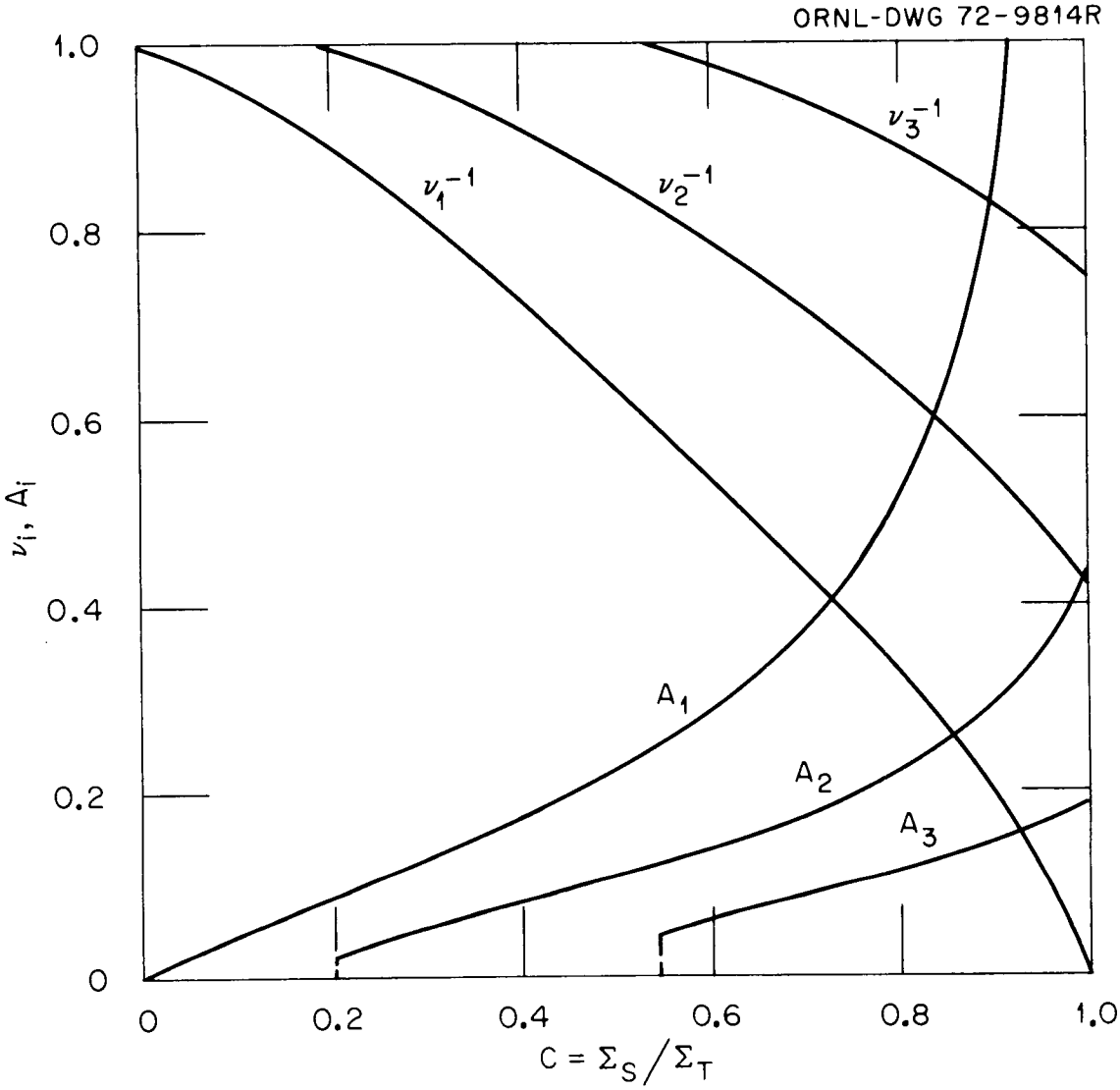

Fig. 8. Discrete Eigenspectrum and Infinite Medium Flux Eigenfunction Coefficients for the ^{238}U 14.1-MeV Angular Distribution as a Function of c, from a P_{39}, f_{14} Calculation.

If we consider a shielding problem with fast neutrons, and consider all inelastic scattering processes to act effectively as absorption near the source energy, then we can expect an eigenspectra similar to those shown with c=0.5, since nonelastic processes are generally less than one half the total cross section at these energies. Thus the spectrum for ^{208}Pb should consist of three discrete roots with about 38% of the flux at x=1 being in other than the largest ν mode. For ^{238}U, there will be a two-root discrete eigenspectrum with 36% of the flux at x=1 in the second mode. All in all, these results together with the knowledge obtained from the gaussian case indicate that multiple roots should play some role in realistic transport problems.

As a final point, the conclusions reached about truncations are again verified in this case. The fluxes for an f_3, f_5, and fully converged f_{39} appearing in Table 5 show that an f_5 is easily sufficient for approximating the largest eigenvalue to three-place precision in the cases shown for either nuclide.

IV. CONCLUSIONS

From the results presented we can draw four conclusions:

1. The strongest and possibly most important practical result to come out of the study is that low-order truncations of the angular distribution yield quite satisfactory monoenergetic scalar fluxes for shielding purposes. In the worst case [a $\delta(\mu-1)/2\pi$ scattering anisotropy] fluxes from a plane isotropic source were found to be within a few percent of the rigorous values over a 10 mfp range with truncation as low as f_3. This result can be extended, by noting that even for this worst anisotropy, an order of magnitude increase in the accuracy of the scalar flux is obtained by simply going to an f_5 truncation. All other anisotropies investigated yielded better results with even lower-order truncations and converged faster to the final answer with the addition of higher-order f_ℓ terms.

Table 5. Discrete Eigenspectra for ^{238}U 14.1 MeV and ^{208}Pb 14.5 MeV Angular Distributions as a Function of c and Highest Order f_ℓ used in P_{39}-Approximation Calculation

^{208}Pb	C=0.5	c=0.8
f_3 (P-39)	ν_1 = 1.4819	ν_1 = 2.7237 ν_2 = 1.1641
f_5 (P-39)	ν_1 = 1.4969 ν_2 = 1.0771	ν_1 = 2.7276 ν_2 = 1.3995
f_{39}(P-39)	ν_1 = 1.4978 ν_2 = 1.1490 ν_3 = 1.0180	ν_1 = 2.7276 ν_2 = 1.4413 ν_3 = 1.1574
^{238}U	c=0.5	c=0.8
f_3 (P-39)	ν_1 = 1.5405	ν_1 = 2.9758 ν_2 = 1.2587
f_5 (P-39)	ν_1 = 1.5590 ν_2 = 1.1044	ν_1 = 2.9819 ν_2 = 1.5277
f_{39} (P-39)	ν_1 = 1.5598 ν_2 = 1.1527	ν_1 = 2.9819 ν_2 1.5519 ν_3 =1.1134

2. With respect to an understanding of the transport process with highly anisotropic scattering, we can certainly conclude that it is both possible and likely for multiple diffusion-type modes to exist in some shielding situations. The contribution of the additional modes and their number increases with increased forward-peaking of the angular distribution and c value of the medium.

3. Unexpectedly, the multiple discrete modes do make a significant contribution to the scalar flux at relatively large distances from the source plane in the infinite media cases studied. Contributions for these additional modes as large as 30% of the total scalar flux for moderately deep-penetration problems (1 to 5 mfp) were found and these results appear to be the rule rather than an exception with highly forward-peaked angular distributions.

4. As for a method of calculating these multiple discrete eigenvalues, we found that a P_L-approximation of sufficiently high order ($L \sim 39$) is a very efficient and accurate method, even in cases involving large numbers of roots.

A convincing mathematical argument can be made to support the first of these conclusions by examining the discrete eigenvalue equation, Eq. (3). Upon close inspection it is easy to show that the dominant factor in each term of the series is $Q_\ell(\nu)$, which for convenience is plotted as a function of ℓ and ν in Fig. 9. Here, we see that for ν values greater than 1.05 the higher order ℓ terms decrease quite rapidly in magnitude. Above $\ell=5$, for ν not too close to unity, the $Q_\ell(\nu)$'s are not more than third or fourth order correction terms to $Q_o(\nu)$. Therefore, barring pathological cases where the $\phi_{\nu\ell}$'s dominate the series of Eq. (3), [the $\phi_{\mu\ell}$'s representing the angular distribution of flux for each ν eigenmode], we see that the $Q_\ell(\nu)$'s will decrease rapidly and cause an early truncation of the series.

While a mathematical explanation of the success of low-order truncations is relatively easy, the problem of understanding the physical meaning behind the conclusions reached about transport in multiple diffusion modes

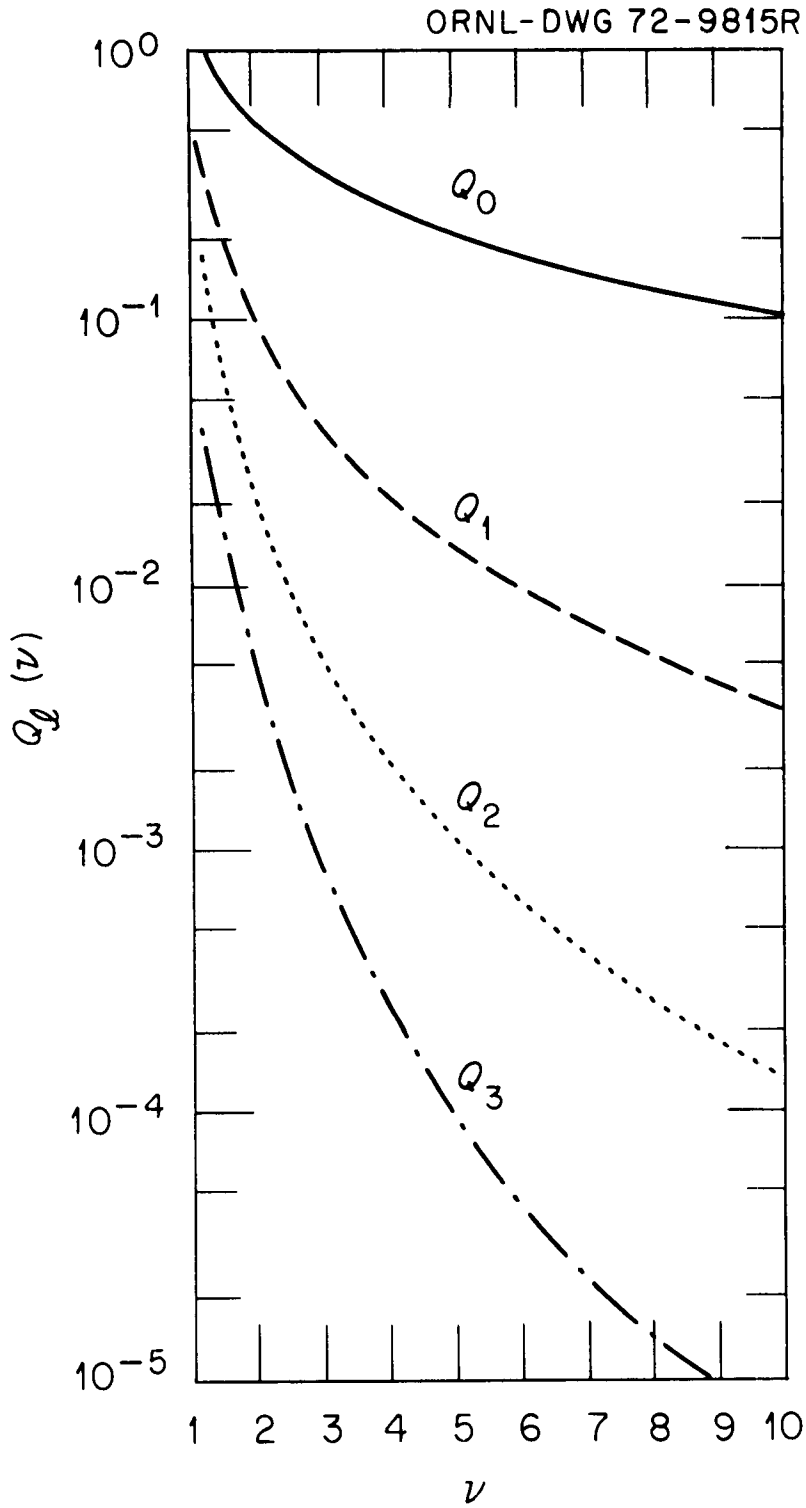

Fig. 9. Legendre Functions of the Second Kind $Q_\ell(\nu)$ as a Function of ν.

is most difficult. The fact that they exist and contribute significantly to transport in realistic situations is clear from the results. Why more than one discrete mode is necessary in any particular problem and the physical role played by such modes in transport is far less clear.

Without really resolving this dilemma, some light can be shed on the problem by looking at these multiple modes in a somewhat novel way. Specifically, let us deal with the quantity $\bar{\mu}_\nu$ defined as follows:

$$\bar{\mu}_{\nu_j} \equiv (1-c)\nu_j \tag{12}$$

such that $|\bar{\mu}_{\nu_j}|<1$. The average quantity is identically equal to the first angular moment, $\phi_{\nu_j 1}$, of the angular flux in ν_j^{th} eigenmode and is thus precisely the average cosine of the angular distribution in this mode.

If the eigenmode solutions for the x>0 flux from a plane source are recast in terms of $\bar{\mu}_{\nu_j}$ we get:

$$\psi(z,\mu) = \sum_{J=1}^{J} A_{\nu_j} \phi_{\nu_j}(\mu)\, e^{-(\Sigma_A z/\bar{\mu}_{\nu_j})} + \int_0^1 A(\nu)\, \phi(\nu,\mu)\, e^{-\Sigma_S z/\nu}\, e^{-\Sigma_A z/\nu}\, d\nu \tag{13}$$

where $\phi_{\nu_j}(\mu)$ and $\phi(\nu,\mu)$ are the discrete and continuum eigenfunctions respectively.

We see from Eq. (13) that both the continuum and discrete eigenmodes have an unscattered flux-type behavior (both ν and the $\bar{\mu}_{\nu_j}$'s have the same range of values as μ), with Σ_A playing the role of a total cross section. Since the only physical decay of the flux in any system comes

from the absorption of neutrons in transport, scattering collisions merely result in a redistribution of the neutrons with respect to angle. Thus each $\bar{\mu}_{\nu_j}$ represents an average angle cosine around which neutrons in the ν_j^{th} discrete mode will transport with the flux decaying only as a result of absorption. The angular redistribution effect is represented in this interpretation by the relative decrease in the magnitude of the continuum modes and a change in their angular distribution with increasing z [as measured by $A(\nu)\, e^{-\Sigma_S z/\nu}\, \phi(\nu,\mu)$]. The net effect of scattering events in transport thus appears as an increase in the proportion of neutrons in the discrete equilibrium modes. As such, this effect is directly related to the probability of scattering in the νth mode through the $e^{-\Sigma_S z/\nu}$ term in the continuum. The eventual asymptotic behavior of the flux can be characterized by discrete mode equilibrium transport with average angular cosines given by the $\bar{\mu}_{\nu_j}$'s and decaying with respect to the absorption cross section Σ_A only. Multiple roots in this interpretation appear to be the result of more complicated equilibrium angular fluxes which must be represented by more than one average angular mode. One might speculate that in multiple discrete mode transport a number of independent equilibrium angular modes are set up as a result of the effect of multiple scattering and the particular scattering anisotropy on the initial angle a particle entered the medium. Clusters of initial angles might contribute to particular asymptotic modes in such an interpretation.

From an overall point of view these conclusions and interpretations lead us to speculate that in highly scattering media with highly anisotropic scattering, diffusion theory will have great difficulties in representing the scalar flux. The multiple mode contribution to transport can never successfully be represented by a theory which allows for only one discrete mode. Since transport proceeds via multiple modes out to reasonably large distances, diffusion theory should fail in such deep-penetration problems. To take care of just such cases, however, our results indicate that no more than a few additional terms in the Legendre expansion of the scattering kernel should be necessary to improve the results substantially.

As a final point, it should be noted that it should be possible to see multiple modes in an experimental situation if the experiment were carefully designed. In particular, the kind of anisotropy and discrete eigenspectrum found in ^{208}Pb at high energies indicates that this nuclide can be used successfully to experimentally identify such modes. One could, for instance, imbed a high energy neutron source in a thick slab of lead to simulate a point source in an infinite medium. The 14.1-MeV neutrons available from the D-T reaction is suitable for this purpose. A measurement could then be made to determine the scalar flux at several spatial distances from the source plane. The existence of multiple discrete transport modes could then be established by the success of a number of exponentials, rather than just one, in fitting the observed spatial variation of the flux. A quantitative comparison of the actual values of the exponential decay constants and the appropriate discrete eigenvalues would add additional information for verification on this score.

Care must be taken to use a coarse energy resolution detection system, so as to measure the flux averaged over a few alpha regions in energy (i.e., $\Delta E/E$ should be a multiple of $1 - [(A-1)/(A+1)]^2$, where A is the atomic mass of lead). Since the effects of leakage out of the measured energy range due to slowing down effects will increase the effective absorption cross section for this group, the group should be wide enough so that an effective c value close to 0.5 will result. This lower limit to c will ensure the existence of well separated multiple discrete flux modes. A 500- to 1000-keV range around 14 MeV should suffice for this purpose. The effective scattering anisotropy for the group is not a concern here since it approaches the real anisotropy at these energies as the group gets wider. For a smaller group the effective anisotropy in fact becomes more forward peaked since back scattering events would cause the neutron to lose too much energy and remove it from the group.

REFERENCES

1. E. Amaldi and E. Fermi, Phys. Rev. 50, 899 (1936).

2. R. E. Marshak, Rev. Mod. Phys. 19, 185 (1947).

3. M. Verde and G. G. Wick, "Some Stationary Distributions of Neutrons in an Infinite Medium," Phys. Rev. 71, 852 (1947).

4. B. Davison, AERE T/R 590 (1950).

5. B. Davison, Neutron Transport Theory, Oxford University Press (1958).

6. J. R. Mika, Nucl. Sci. Eng. 11, 415 (1961).

7. A. M. Jacobs, "Solution of Monoenergetic Neutron Transport Equation," Thesis, Pennsylvania State University (1963).

8. K. M. Case, "Elementary Solutions of the Transport Equation," Ann. Phys. 9, 1 (1960).

9. H. Goldstein, "Survey of Theoretical Studies at Columbia University on Fast Neutron Transport in Iron," Trans. Am. Nucl. Soc. 13, 262 (1970).

10. I. W. Busbridge, Astrophys. J. 149, 195 (1967).

11. H. G. Kaper et al., "One Speed Transport Theory with Anisotropic Scattering," Report TW-65, Mathematisch Institut, University of Groningen-Netherlands.

12. H. C. Van de Hulst, "The Spectrum of the Anisotropic Transfer Equation," Astron. & Astrophys. 9, 366 (1970).

13. K. M. Case and P. F. Zweifel, Linear Transport Theory, Addison-Wesley Publishing Company, Massachusetts (1967).

14. M. Abromowitz and I. A. Stegun, Handbook of Mathematical Functions, p. 332, National Bureau of Standards (1964).

15. "Compilation, Evaluation, and Reduction of Neutron Differential Scattering Data," NAA-SR-11980, Vol. IV (1967).

16. E. Gelbard et al., "Iterative Solutions to P-L and Double P-L Equations," Nucl. Sci. & Eng. 5, 1 (1959).

17. J. H. Wilkinson, The Algebraic Eigenvalue Problem, Oxford University Press, Oxford, 1965.

INTERNAL DISTRIBUTION

1-3. L. S. Abbott
4. R. G. Alsmiller, Jr.
5. D. E. Bartine
6. G. P. Cavanaugh
7-8. C. E. Clifford
9. S. N. Cramer
10. F. L. Culler
11. W. W. Engle, Jr.
12. G. F. Flanagan
13. N. M. Greene
14. W. O. Harms
15. J. L. Lucius
16. R. E. Maerker
17. F. C. Maienschein
18. G. W. Morrison
19. F. R. Mynatt
20-29. E. M. Oblow
30. J. V. Pace, III
31. R. W. Peelle
32. S. K. Penny
33. F. G. Perey
34. A. M. Perry
35. L. M. Petrie
36. W. A. Rhoades
37. E. G. Silver
38. P. N. Stevens
39. D. B. Trauger
40. D. K. Trubey
41. C. R. Weisbin
42. J. E. White
43. G. E. Whitesides
44. H. Feshbach (consultant)
45. P. F. Fox (consultant)
46. C. R. Mehl (consultant)
47. H. T. Motz (consultant)
48-49. Central Research Library
50. ORNL Y-12 Technical Library Document Reference Section
51-55. Laboratory Records
56. Laboratory Records ORNL RC
57. ORNL Patent Office

EXTERNAL DISTRIBUTION

58-212. Given DNA Radiation Transport Distribution (Updated 3-30-73)
213. Norman Banks, U. S. Army Ballistics Research Laboratory, Aberdeen Proving Ground, Maryland 21005
214. A. R. Buhl, Acting Chief, Core Design Branch, Division of Reactor Research and Development, U. S. Atomic Energy Commission, Washington, D. C. 20545
215. R. Conn, University of Wisconsin, Nuclear Engineering Dept., 1500 Johnson Drive, Madison, Wisconsin 53706
216. D. E. Cullen, Lawrence Livermore Laboratory, Livermore, Calif. 94550
217. N. C. Francis, Knolls Atomic Power Laboratory, General Electric, P. O. Box 1072, Schenectady, N. Y. 12301
218. S. A. W. Gerstl, Argonne National Laboratory, 9700 South Cass Avenue, Argonne, Illinois 60439
219. H. Goldstein, Columbia University, 287A Mudd Building, New York, NY 10027
220. P. Greebler, General Electric Co., Breeder Reactor Development Operation, 310 DeGuigne Drive, Sunnyvale, California 94086
221. J. P. Hamric, Division of Reactor Development and Technology, U. S. Atomic Energy Commission, Washington, D. C. 20545
222. W. H. Hannum, Division of Reactor Research and Development, U. S. Atomic Energy Commission, Washington, D. C. 20545
223. P. B. Hemmig, Division of Reactor Research and Development, U. S. Atomic Energy Commission, Washington, D. C. 20545

224. T. J. Hoffman, Science Applications, Inc., Huntsville, Alabama 35805
225. E. E. Kintner, Division of Research and Development, U. S. Atomic Energy Commission, Washington, D. C. 20545
226. K. O. Laughon, USAEC Site Representative, ORNL
227. P. Soran, Los Alamos Scientific Laboratory, P. O. Box 1663, Los Alamos, New Mexico 87544
228. R. J. Neuhold, Division of Reactor Research and Development, U. S. Atomic Energy Commission, Washington, D. C. 20545
229. Prof. P. F. Pasqua, Department of Nuclear Engineering, University of Tennessee, Knoxville, Tennessee
230. D. R. Riley, U. S. Atomic Energy Commission, Division of Reactor Research and Development, Washington, D. C. 20545
231. W. M. Stacey, Jr., Applied Physics Division, Argonne National Laboratory, 9700 South Cass Avenue, Argonne, Illinois 60439
232. Dr. Leona Stewart, Los Alamos Scientific Laboratory, P. O. Box 1663, Los Alamos, New Mexico 87544
233. Phil Young, Los Alamos Scientific Laboratory, P. O. Box 1663, Los Alamos, New Mexico 87544

234-235. Technical Information Center (TIC)

236. Research and Technical Support Division ORO